A STUDY ON COMPLICATED ROLL MOTION OF A SHIP EQUIPPED WITH AN ANTI-ROLLING TANK

Harukuni Taguchi, Hiroshi Sawada and Katsuji Tanizawa
National Maritime Research Institute (JAPAN)

Abstract

Nonlinear roll motion of a ship with a Frahm type anti-rolling tank (ART) onboard is investigated experimentally and numerically. The model experiment was conducted for two loading conditions, namely normal stability condition and poor stability condition, in regular beam waves. It is found that the model ship with the ART in poor stability condition can exhibit irregular and complicated roll motion even in regular waves. In order to further investigate complicated roll motion of a ship with an ART in such condition, time-domain simulations with nonlinear equations of coupled motions of rolling of a ship and fluid transfer in the tank were carried out. Bifurcation diagrams with changing forcing frequency, "Ω", and forcing amplitude, "A", which correspond to wave frequency and wave steepness respectively, show that complicated roll motion exists in a wide range of parameters in low frequency region. This is also confirmed in a control parameter plane, which consists of Ω and A. However in high frequency region, where complicated roll motion was observed in the model experiment, such behaviour of a ship has not been found. This implies that the numerical investigation reveals only one of features of a ship with an ART in poor stability condition and that further investigation is necessary to understand overall behaviour of such ship in waves.

1. INTRODUCTION

As roll stabilization device, anti-rolling tanks are fitted to many ships. An anti-rolling tank utilises the fluid motion in the tank for decreasing the roll motion of the ship. Passive type anti-rolling tanks are designed to have the same natural period for the fluid transfer in the tank as that for the rolling of the ship, but ninety degrees out-of-phase to the roll motion. So such anti-rolling tanks achieve maximum effect in the resonance condition. However for a ship like fisheries training ship, whose metacentric height (GM) largely varies during operation, a passive type of anti-rolling tank might increase the roll motion, because the resultant natural rolling period deviates from the designed one. To overcome this drawback, frequency variable type and active control type anti-rolling tanks have been developed.

When an anti-rolling tank is activated, the free surface moment in the tank decreases GM of the ships. Ships fitted with anti-rolling tanks are designed to have sufficient stability with taking the resultant loss of GM into account. However in poor stability condition the resultant loss of GM might lead the ship to dangerous situation. Many investigations so

far (e.g. [1]-[4]) were conducted for effects of anti-rolling tanks on the rolling responses of ships in normal stability condition. However effects of anti-rolling tanks in poor stability condition have not been investigated so much.

Last year authors had a chance to conduct an experiment using a model ship with a Frahm type (U-tube type) anti-rolling tank onboard. Taking this opportunity we measured the roll motion of the model ship in poor stability condition in beam waves. And in order to further study behaviour of a ship in such condition qualitatively, we carried out numerical simulations with nonlinear equations of the coupled motions of rolling of a ship and fluid in an anti-rolling tank. This paper reports the outline of these investigations.

2. MODEL EXPERIMENT

2.1.Outline of the Experiment

Model experiment was conducted in the seakeeping wave tank at National Maritime Research Institute (length: 50.0m, width: 8.0m, depth: 4.5m). A model of a small fishing boat was used. Fig. 1 shows the outline of the model ship and its principal dimensions are shown in Table 1. A Frahm type anti-rolling tank (ART) was attached on the aft deck (see Fig. 1). The outline of the ART is shown in Fig. 2 and Table 2 shows its principal dimensions.

The model ship was placed at the middle of the tank and moored by weak tension cords to keep beam wave condition and to restrict free drift motion (see Fig. 3). The roll, heave and sway motions of the model ship with the ART in regular beam waves were measured by a video tracker system. As the targets for the video tracker small lights were attached at the top and root of the mast (see Fig.1).

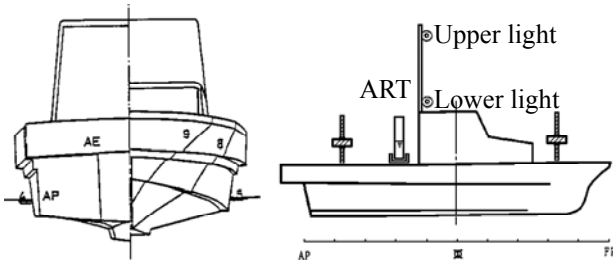

Fig. 1 Model ship used in the experiment

Table 1 Principal dimensions of the model ship

Length (overall)	130 cm
Breadth (overall)	40.8 cm
Draft (overall)	7.5 cm
Displacement	18.18 kg

In the experiment motions of the model ship with the ART both activated and inactivated conditions were measured. Measurements were conducted for a normal stability condition (GM = 2.24 cm with the ART inactivated) and a poor stability condition (GM = 0.74 cm with the ART inactivated). The resultant natural rolling periods were 2.0 sec. for GM = 2.24 cm and 3.7 sec. for GM = 0.74 cm, respectively. So the natural period of rolling in the normal stability condition was the same as that of the ART. In order to investigate global behaviour of the model ship, the wave period, T_w, was changed from 1.0 to 2.6 sec. while the wave height, H_w, was kept constant, H_w = 5 cm. Moreover measurements were also carried out in waves of the period T_w = 2.0 sec. and with increase of the wave height.

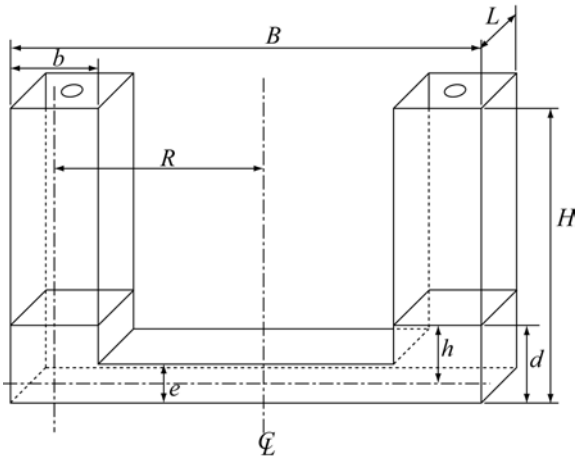

Fig. 2 ART used in the experiment

Table 2 Principal dimensions of ART

Length	L	4.4 cm
Breadth	B	40.4 cm
Breadth of vertical tube	b	7.54 cm
Height	H	10.45 cm
Height of horizontal tube	e	1.3 cm
Water depth	d	2.6 cm
Weight of fluid in ART	W_f	0.28 kg
Natural period of ART	T_{ART}	2.0 sec.

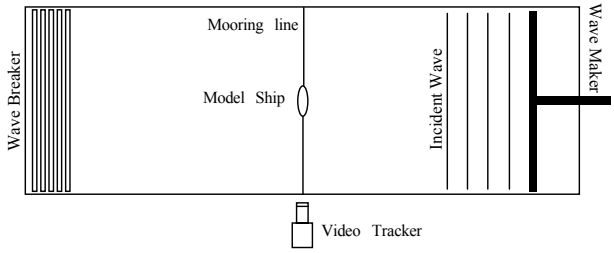

Fig. 3 Experimental setup in the wave tank

2.2.Experimental Results

Normal Stability Condition

Fig. 4 shows the measured rolling amplitudes of the ship in the normal stability condition. The horizontal axis is the ratio between wave frequency and natural rolling frequency and the vertical axis is the rolling amplitude

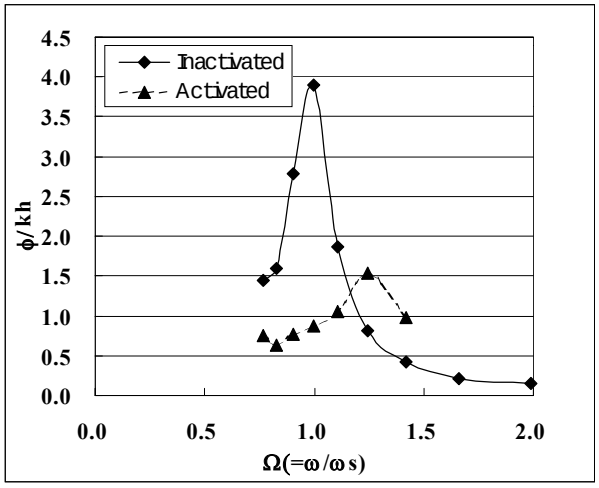

Fig. 4 Rolling responses with the ART activated and inactivated (GM = 2.24 cm)

normalised by the wave slope. In this case typical rolling responses with an ART were obtained because the natural period of rolling was the same as that of the ART. As shown in Fig. 4, the ART reduces rolling amplitude near the resonance frequency (Ω = 1.0) while at higher side region of the resonance frequency the ART gives negative effect and the rolling amplitude is increased.

Poor Stability Condition

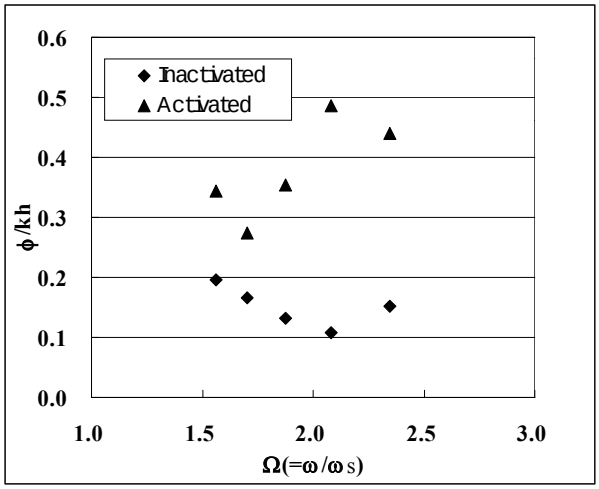

Fig. 5 Rolling responses with the ART activated and inactivated (GM = 0.74 cm)

In the poor stability condition the resultant GM due to the free surface moment in the tank becomes negative, so the model ship is statically balanced with about 9 degrees heeled position in still water. The experiment was started after the model was set to the statically balanced potion in the weather side. In this case the natural period of rolling differs from that of the ART. And the wave periods were set around the natural period of the ART. Fig. 5 shows the measured rolling amplitudes of the ship in the poor stability condition. Because the wave frequencies are out of resonance condition, the rolling responses are small in both the ART activated and inactivated conditions, but negative effect of the ART is seen in all waves.

In order to further investigate behaviour of the model ship with the ART activated in the poor stability condition, measurements with increase of the wave height were carried out. Fig. 6 shows the time histories of measured roll angle in waves of the period T_w = 2.0 sec. with changing the wave height from 5 to 25 cm. For small wave height, H_w = 5 cm and 10 cm, the rolling response is very small. For H_w = 15 cm and 20 cm, the model ship exhibits quite irregular and complicated roll motion around the two static balanced positions in the lee and the weather sides. For H_w = 25 cm roll motion around the lee side static balanced position with the same period as the wave is found.

In Fig. 7 the time history of measured roll angle for H_w = 20 cm in long time duration is shown. The roll motion seems to be chaotic. A similar type of complicated rolling response was observed in numerical simulations with a nonlinear rolling equation for a ship in negative GM without an ART [5][6].

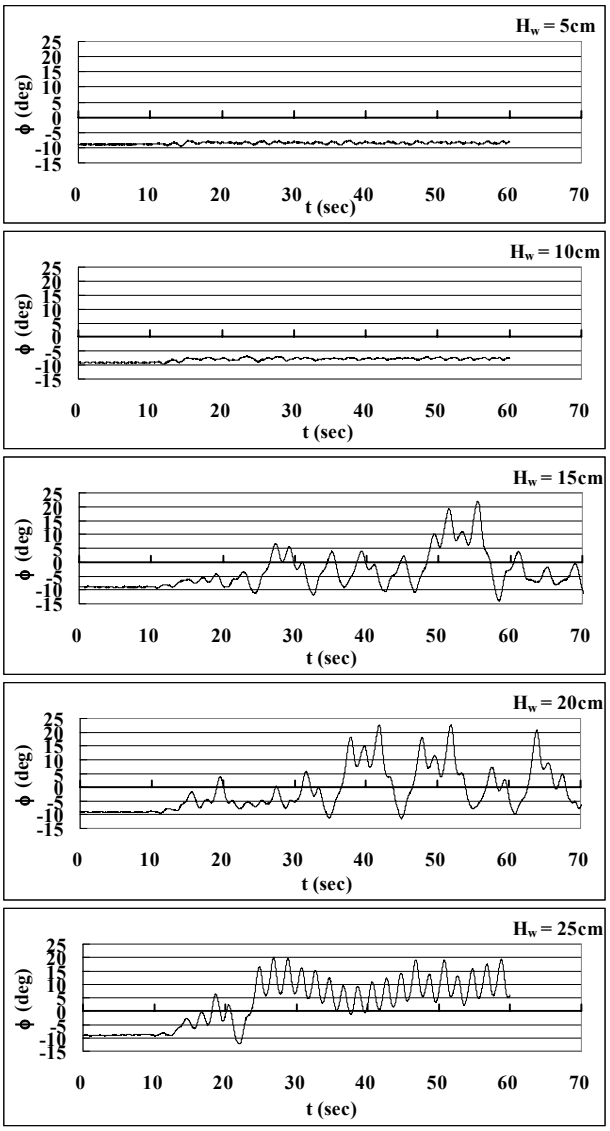

Fig. 6 Measured roll motion of the model ship (T_w = 2.0 sec.)

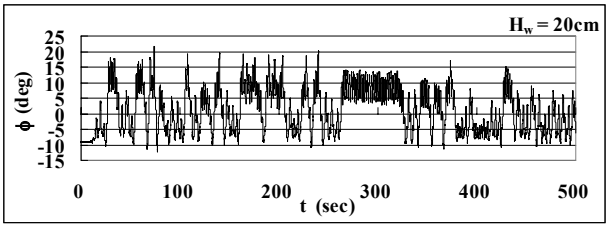

Fig. 7 Measured roll motion of the model ship (T_w = 2.0 sec. and H_w = 20 cm)

3. NUMERICAL INVESTIGATION

In order to investigate global rolling response of a ship with an anti-rolling tank in poor stability condition qualitatively, we carried out numerical simulations with equations of the coupled motions of rolling of a ship and fluid in an anti-rolling tank. In the investigation we treated the coupled motions as a nonlinear dynamical system. In this paper, as the first step of the numerical investigation, we examine the coupled motions with bifurcation diagrams and a control parameter plane where some feature of global rolling response of a ship with an anti-rolling tank may be exhibited.

3.1. Coupled Motions of Rolling of a Ship and Fluid in an Anti-Rolling Tank

Utilising coordinate system shown in Fig. 8, linear coupled equations of motions of rolling of a ship and fluid in an anti-rolling tank can be expressed as follows [7].

$$J_s\frac{d^2\phi}{dt^2}+B_s\frac{d\phi}{dt}+K_s\phi+J_{st}\frac{d^2\theta}{dt^2}+K_t\theta=K_s\varphi \qquad (1)$$

$$J_{st}\frac{d^2\phi}{dt^2}+K_t\phi+J_t\frac{d^2\theta}{dt^2}+B_t\frac{d\theta}{dt}+K_t\theta=K_t\varphi \qquad (2)$$

where ϕ is the ship roll angle, θ is the tank water slope angle, φ is the wave slope angle, t is the time, J_s is the moment of inertia of ship, B_s is the damping coefficient of ship, K_s is the restoring coefficient of ship: W·GM (W is the displacement of ship), J_t is the moment of inertia of fluid in the tank, B_t is the damping coefficient of fluid in the tank, K_t is the restoring coefficient of fluid in the tank: $W\cdot GG_0$ (GG_0 is the virtual rise of the centre of gravity due to free surface in the tank), J_{st} is the coupling coefficient of ship and fluid in the tank.

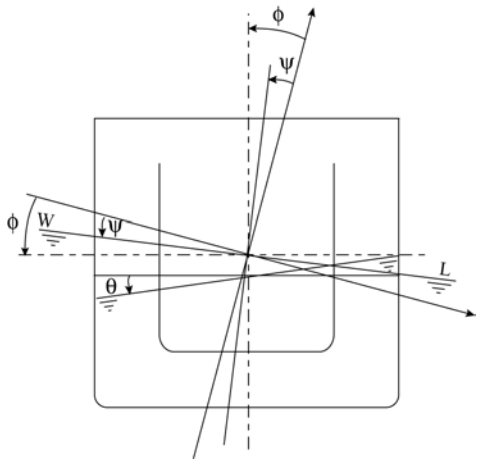

Fig. 8 Coordinate system

Moreover the wave slope angle, φ, is generally expressed in following time dependent form.

$$\varphi = ak\sin\omega t \qquad (3)$$

where a is the wave amplitude, k is the wave number and ω is the wave frequency.

In order to examine the global rolling response in poor stability condition, it was considered that nonlinearity in restoring moment of a ship should be included in the equations of coupled motions. In this investigation we used the following approximated expression for a stability curve of a ship in poor stability condition (slightly positive GM).

$$WGZ = K_s\phi\left\{1+r\left(\frac{\phi}{\phi_v}\right)^2-(1-r)\left(\frac{\phi}{\phi_v}\right)^4\right\} \qquad (4)$$

where ϕ_v is the vanishing angle of stability and K_s is defined as mentioned above: $K_s=W\cdot GM$. If the value of r is specified, both GZ_{max} and ϕ_{max} are determined automatically in this form, however typical characteristics of nonlinearity in restoring moment can be obtained qualitatively.

Using this expression in restoring term, equation (1) is rewritten as follows.

$$J_s \frac{d^2\phi}{dt^2} + B_s \frac{d\phi}{dt} + K_s\phi\left\{1 + r(\frac{\phi}{\phi_v})^2 - (1-r)(\frac{\phi}{\phi_v})^4\right\} + J_{st}\frac{d^2\theta}{dt^2} + K_t\theta = K_s\varphi \qquad (5)$$

Normalizing each angle by ϕ_v and the time by ω_s, the natural rolling frequency of a ship ($\omega_s = (K_s/J_s)^{1/2}$), and using time dependent form of the wave slope, equations (5) and (2) are converted to

$$\frac{d^2\phi'}{ds^2} + \kappa\frac{d\phi'}{ds} + \phi'\left\{1 + r\phi'^2 - (1+r)\phi'^4\right\} + \nu_{st}\frac{d^2\theta'}{ds^2} + \lambda\theta' = A\sin\Omega s \qquad (6)$$

$$\frac{\nu_{st}}{\nu_t}\frac{d^2\phi'}{ds^2} + \frac{\lambda}{\nu_t}\phi' + \frac{d^2\theta'}{ds^2} + \mu\sqrt{\frac{\lambda}{\nu_t}}\frac{d\theta'}{ds} + \frac{\lambda}{\nu_t}\theta' = \frac{\lambda}{\nu_t}A\sin\Omega s \qquad (7)$$

where $s = \omega_s t$, $\phi' = \phi/\phi_v$, $\theta' = \theta/\phi_v$, $\kappa = B_s/(J_s\cdot\omega_s)$, $\lambda = K_t/K_s$, $\nu_{st} = J_{st}/J_s$, $\nu_t = J_t/J_s$, $\mu = B_t/(J_t\cdot\omega_t)$, $A = ak/\phi_v$, and $\Omega = \omega/\omega_s$.

Table 3 Values of fixed coefficients used in the numerical investigation

κ	0.60
μ	0.26
λ	1.5
r	6.0
ν_{st}	0.0
ν_t	0.37

In the numerical investigation coefficients A, the forcing amplitude, and Ω, the forcing frequency, were varied while the other coefficients were fixed. The values of fixed coefficients are summarized in Table 3. The values of κ, μ, ν_{st}, and ν_t, are close to those of the experiment. And the values of r is determined by the least square approximation of stability curve of the model ship. Moreover in order to investigate an extremely poor stability condition, λ was set to 1.5.

For A□0, which corresponds to still water, from equations (6) and (7) we get the following relations in steady state.

$$\phi'\left\{1 + r\phi'^2 - (1+r)\phi'^4\right\} + \lambda\theta' = 0 \qquad (8)$$

$$\phi' + \theta' = 0 \qquad (9)$$

Substituting equation (9) into equation (8) gives us equation (10).

$$(1-\lambda)\phi' + r\phi'^3 - (1+r)\phi'^5 = 0 \qquad (10)$$

From equation (10) we can understand that when λ is larger than 1, the upright condition becomes unstable and the ship is statically balanced in heeled condition.

3.2.Bifurcation Diagrams

Fig. 9 shows a bifurcation diagram for $A = 0.2$ with changing Ω. This bifurcation diagram is obtained as follows. First we solve the equations (6) and (7) numerically with the 5th–order Runge-Kutta method for $\Omega = 0.01$ with the initial condition, $\phi'(0) = \phi_0$, $\theta'(0) = -\phi_0$, $\phi'(0)/ds = d\theta'(0)/ds = 0$, which corresponds to the statically heeled condition in still water. After the transient responses die out, we plot the responses at every one forcing cycle with the same phase angle as much as 20 cycles. Then increasing Ω by small amount, $\Delta\Omega = 0.01$, we continue the time integration and after extinction of the transient responses, we similarly plot the responses at every one cycle. By continuing these procedures the bifurcation diagram, Fig. 9, is obtained. It is considered that a bifurcation diagram with changing Ω corresponds to steady state rolling response obtained by a model experiment with the wave steepness kept constant but the wave frequency gradually changed. And in this case

A = 0.2 corresponds to the wave steepness of about 1/23 in the model experiment mentioned in section 2.

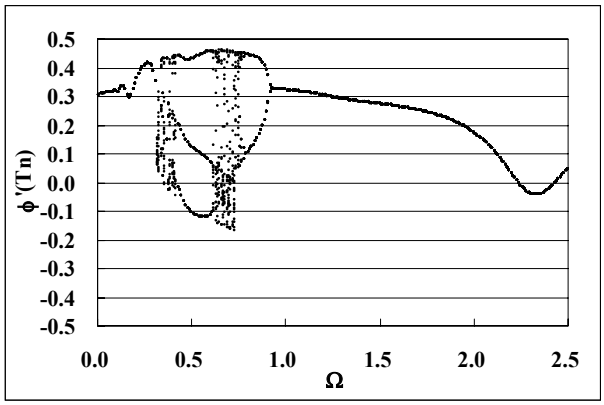

Fig. 9 Bifurcation diagram with changing Ω (A = 0.20)

From Fig. 9 it is found that in low frequency region, 0.24 < Ω < 0.93, very complicated roll motion seems to exist. To illustrate these complicated rolling more clearly, time histories of ϕ', the ship roll angle, and θ', the tank water slope angle, together with phase portraits in (ϕ'-d ϕ'/ds) and (θ'-dθ'/ds) for Ω = 0.4 and 0.7 are shown in Fig. 10. Roll motions for Ω = 0.4, 0.7 might be chaotic.

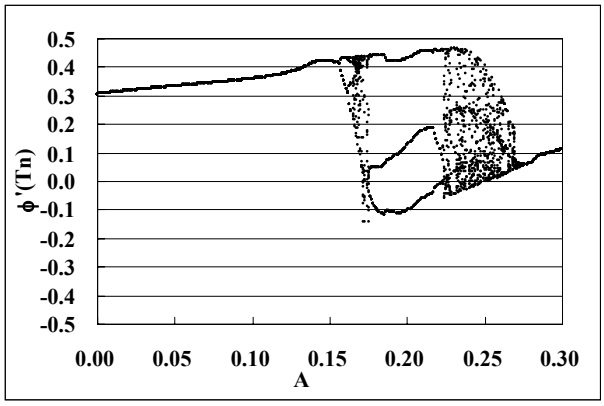

Fig. 11 Bifurcation diagram with changing A (Ω = 0.5)

In the model experiment complicated roll motions were observed at relatively high wave frequency, which corresponds to Ω = 1.85, however under the condition for Fig. 9 only simple roll motion with the same period as the forcing period is found in high frequency region.

Fig. 11 shows bifurcation diagram for Ω = 0.5 with changing A. A bifurcation diagram with changing A is consider to correspond to steady state rolling response obtained by a model experiment with keeping the wave frequency constant but changing the wave height gradually. From Fig. 11 it is found that rolling response changes in very complicated way as the forcing amplitude increases. The period doubling bifurcation begins at about A = 0.16 and it leads to chaotic roll motion. As the forcing amplitude is increased further, chaotic motion changes to a subharmonic motion of order 3 at about A = 0.175 and this subharmonic motion continues to exist until the forcing amplitude reaches at about 0.22. Then the roll motion becomes chaotic again and at about A = 0.28 it changes to simple motion with the same period as the forcing period.

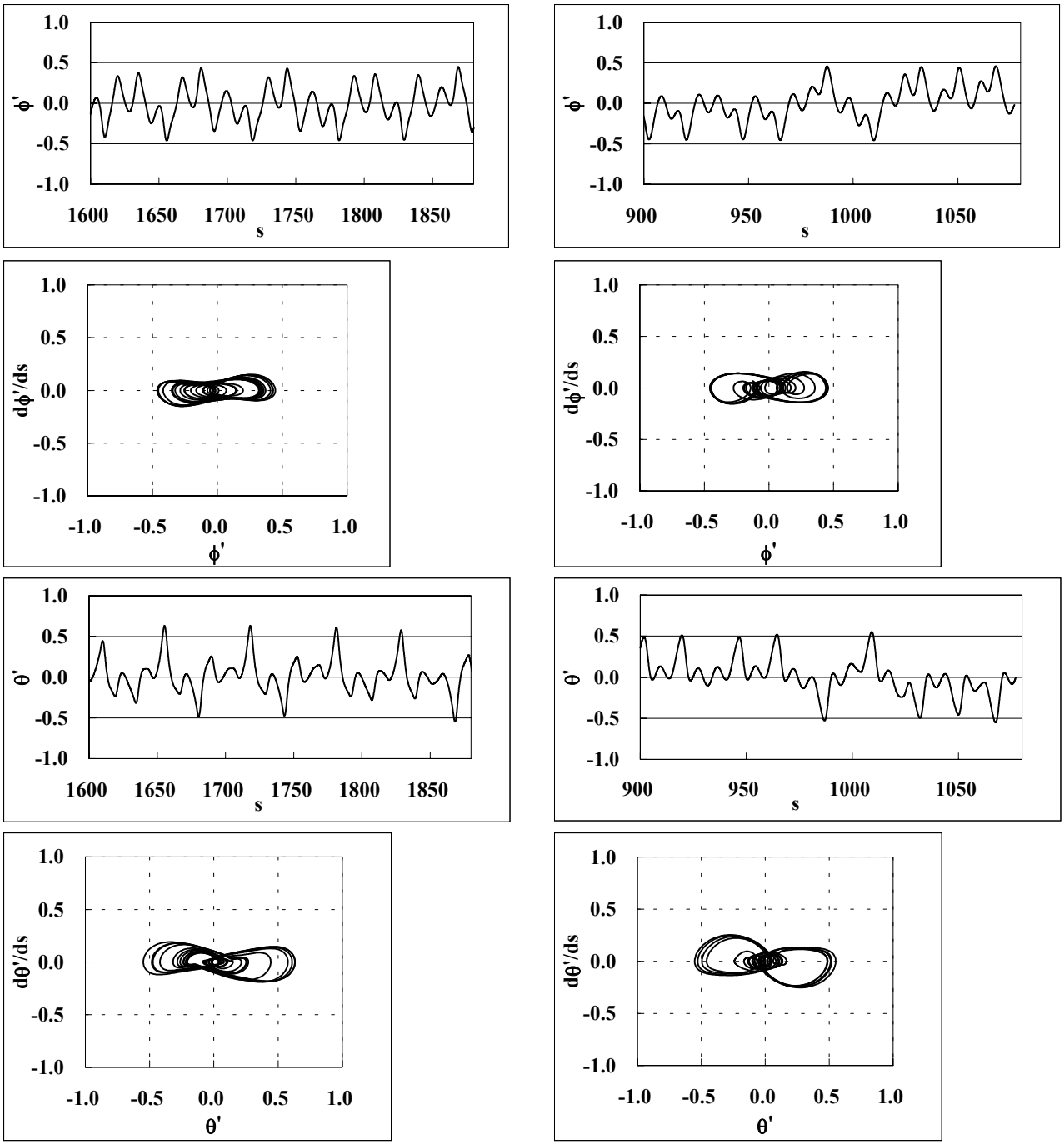

(a) $\Omega = 0.4$ (b) $\Omega = 0.7$

Fig. 10 Time histories of ϕ', the ship roll angle, phase portraits in (ϕ'-d ϕ'/ds), time histories of θ', the tank water slope angle, and phase portraits in (θ'-dθ'/ds) obtained by numerical simulation (from top)

3.3. Complicated Roll Motion Region in a Control Plane

To illustrate the parameter dependency of complicated roll motion, a control plane, which consists of Ω and A, control parameters of the equations (6) and (7), is divided into two regions as shown in Fig. 12. In Fig. 12 parameters Ω and A in black region leads to complicated rolling while parameters in white region lead to simple motion with the same period as the forcing period. This figure is obtained as follows. We solve the equations (6) and (7) with 5th-order Runge-Kutta method from the initial condition, which corresponds to the statically heeled condition in still water, $\phi'(0) = \phi_0$, $\theta'(0) = -\phi_0$, $\phi'(0)/ds = d\theta'(0)/ds = 0$, up to 120 forcing cycles for a combination of Ω and A and examine whether the last 20 cycle roll motion exhibits complicated feature or not. By repeating these procedures for parameters at fine grid points of the control plane, we obtain Fig. 12. The control plane in Fig. 12 is divided into 250 x 300 grid points.

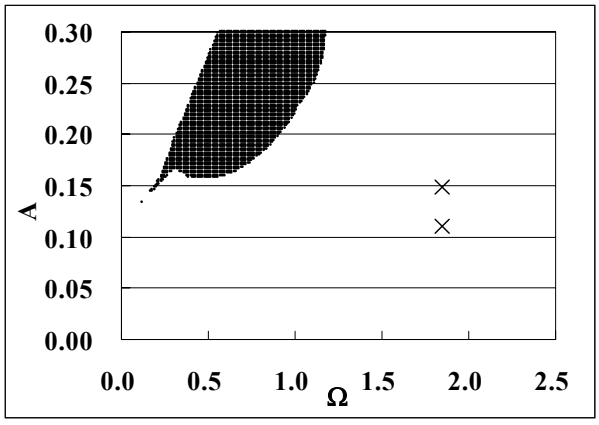

Fig. 12 Complicated roll motion region in Ω-A control plane (×: in the model experiment)

From Fig. 12 it is found that complicated rolling exists in a wide range of parameters Ω and A. And as seen in the bifurcation diagram with changing A, Fig. 8, there is the limit for complicated rolling in larger forcing amplitude side.

In Fig. 12 the conditions, in which complicated roll motion was observed in the model experiment, are shown with ×. These conditions are out of the complicated roll motion region defined by the numerical investigation.

In general, nonlinear dynamical system can exhibit more than one type of response for the same parameters depending on the initial condition. So the region of complicated rolling in the control plane might be changed for the different initial conditions. To clarify the dependency on initial condition investigation into the initial value planes obtained with similar procedures to the control plane is necessary.

3.4. Some Discussions on Numerical Investigation

As shown in Figs 9-12 it is found that roll motion of a ship with an ART, expressed by equations (6) and (7) could exhibit complicated response in a wide range of control parameters Ω and A, which correspond to the wave frequency and the wave steepness, in relatively low frequency region.

However complicated roll motion in high frequency region, which was observed in the model experiment, is not found in this numerical investigation.

This implies that only one of features of roll motion of a ship with an ART in poor stability condition is clarified with this numerical investigation.

In order to understand overall behaviour of such ship, further numerical investigation including examination of dependency of

complicated rolling on the parameter λ and on the initial condition is necessary.

4. CONCLUSION

Roll motion of a ship with a Frahm type anti-rolling tank onboard was investigated experimentally and numerically.

As a result it is found that the model ship with poor GM might exhibit complicated behaviour in beam waves of relatively high frequency compared with the natural frequency of rolling. Measured data shows that the roll motion in such condition might be chaotic.

Numerical investigation with equations of the coupled motions of rolling of a ship and fluid in an anti-rolling tank shows that roll motion in poor stability condition could exhibit complicated response in a wide range of control parameters Ω and A, which correspond to the wave frequency and the wave steepness, in relatively low frequency region. However in the numerical investigation only simple roll motion with the same period as the forcing period is found in high frequency region.

In order to deepen our understandings of the behaviour of a ship with an ART in poor stability condition, further investigation should be continued.

5. ACKNOWLEDGEMENTS

The experiment of this work was conducted as a funded research from an ART maker Stabilo Corporation. The authors would like to acknowledge the representative director Mr. N. Matsumura for his sponsorship to this work.

6. REFERENCE

[1]. Y. Watanabe: On the Design of Anti-Rolling Tanks, Journal of the Society of Naval Architects of Japan, Vol. 46, pp 125-153, 1930 (in Japanese).

[2]. J. H. Chadwick: On the Stabilization of Roll, Transactions of the Society of Naval Architects and Marine Engineers, Vol. 63, pp 237-280, 1955.

[3]. G. J. Goodrich: Development and Design of Passive Roll Stabilisers, Transactions of the Royal Institution of Naval Architects, Vol. 111, pp 81-95, 1969.

[4]. Y. Takaishi: A Model Experiment on the Effect of an Anti-Rolling Tank of Ship in Oblique Seas, Journal of the Kansai Society of Naval Architects, Japan, Vol. 141, pp 45-53, 1971 (in Japanese).

[5]. M. Kan and H. Taguchi: Chaos and Fractals in Loll Type Capsize Equation, Transactions of the West-Japan Society of Naval Architects, No. 83, pp 131-149, 1992 (in Japanese).

[6]. K. Tanizawa and S. Naito: An Application of Fully Nonlinear Numerical Wave Tank to the Study of Chaotic Roll Motions, International Journal of Offshore and Polar Engineering, Vol. 9, No. 2, pp 90-96, 1999.

[7]. S. Watanabe: Reduction of Rolling, (2) Anti-Rolling Tank, Proceedings of the 1st Symposium on Seakeeping, The Society of Naval Architects of Japan, pp 158-179, 1969 (in Japanese).